https://ntrs.nasa.gov/search.jsp?R=19680014138 2020-03-12T10:37:47+00:00Z

General Disclaimer

One or more of the Following Statements may affect this Document

- This document has been reproduced from the best copy furnished by the organizational source. It is being released in the interest of making available as much information as possible.

- This document may contain data, which exceeds the sheet parameters. It was furnished in this condition by the organizational source and is the best copy available.

- This document may contain tone-on-tone or color graphs, charts and/or pictures, which have been reproduced in black and white.

- This document is paginated as submitted by the original source.

- Portions of this document are not fully legible due to the historical nature of some of the material. However, it is the best reproduction available from the original submission.

Produced by the NASA Center for Aerospace Information (CASI)

PB 177 141

PLANE-FLAME SIMULATION OF THE WAKE BEHIND AN INTERNALLY PROPELLED VEHICLE. PART 2. SIMULATION OF A SUBSONIC VEHICLE BY A HEAT SOURCE

John H. Skinner, Jr.

Rensselaer Polytechnic Institute
Troy, New York

July 1967

PB 177141

RENSSELAER POLYTECHNIC INSTITUTE

KNOWLEDGE AND THOROUGHNESS

1824

PROJECT TUBEFLIGHT

J. H. SKINNER

VEHICLE WAKE SIMULATION
PART 2

Reproduced by the
CLEARINGHOUSE
for Federal Scientific & Technical
Information Springfield Va. 22151

TR AE 6705

PLANE-FLAME SIMULATION OF THE WAKE BEHIND AN INTERNALLY PROPELLED VEHICLE

PART 2
SIMULATION OF A SUBSONIC VEHICLE BY A HEAT SOURCE

by
John H. Skinner, Jr.

This research was supported in part by a NASA Traineeship and in part by the United States Department of Commerce Contract No. C-117-66 (Neg.)

This paper is taken from part of a thesis to be submitted in partial fulfillment of the requirements for the degree of Doctor of Philosophy in the Department of Aeronautical Engineering and Astronautics at Rensselaer Polytechnic Institute

DEPARTMENT OF AERONAUTICAL ENGINEERING AND ASTRONAUTICS
RENSSELAER POLYTECHNIC INSTITUTE
TROY, NEW YORK

JULY 1967

TABLE OF CONTENTS

ABSTRACT

The development of the flow field about an internally-propelled vehicle in steady motion at subsonic speed in a tube is analyzed by the method of characteristics. The vehicle is simulated by a heat source releasing heat at a constant rate and moving through an infinite duct at a constant subsonic velocity. Friction and heat transfer are accounted for, and the characteristic equations are integrated numerically employing a high-speed computer.

In a vehicle-fixed frame of reference the induced flow field is initially steady, but friction and heat transfer soon cause it to become nonsteady. As time progresses, the nonsteady effects slowly decay and the flow field asymptotically approaches a steady state.

SYMBOLS

a speed of sound

$A = a/a_o$ nondimensional speed of sound

c_p specific heat at constant pressure

$C_f = \frac{f g \pi}{u|u|}$ friction factor

f friction force per unit weight

g gravitational constant

h film coefficient of heat transfer

$\dot{j}$ flame heat release per unit mass of gas burned

$J = \frac{(\gamma^2-1) 2 g \dot{j}}{a_o^2}$ nondimensional flame heat release per unit mass of gas burned

$\dot{J} = J\left(\frac{\rho_u N_u}{\rho_o a_o}\right)$ nondimensional time rate of heat release of flame

K conduction multiplier

L_o reference length

M Mach number

p pressure

$P = \frac{2}{\gamma-1} A + U$

$Q = \frac{2}{\gamma-1} A - U$ Riemann variables

R perfect gas constant

π tube radius

$\bar{\pi} = \pi/L_o$ nondimensional tube radius

s entropy per unit mass

$S = s/\gamma R$ nondimensional entropy

t time

T temperature

u velocity relative to tube walls

$U = u/a_o$ nondimensional velocity

v velocity relative to heat source

x distance along tube axis

γ ratio of specific heats

$\xi = x/L_o$ nondimensional distance along tube axis

ρ density

$\tau = \frac{t a_o}{L_o}$ nondimensional time

Superscript

o stagnation conditions

Subscript

b conditions immediately behind heat source

f heat source

o free stream ambient

s1 shock 1

s2 shock 2

u conditions immediately ahead of heat source

v vehicle

Derivatives

$\frac{D}{Dt} = \frac{\partial}{\partial t} + u\frac{\partial}{\partial x}$ substantial derivative

$\frac{\delta_\pm}{\delta t} = \frac{\partial}{\partial t} + (u \pm a)\frac{\partial}{\partial x}$ derivatives in characteristic directions

I. INTRODUCTION

This report presents the second part of a study[1] of the effects of friction and heat transfer on the flow induced by an internally-propelled vehicle traveling in a tube. This part of the study deals specifically with vehicles moving at subsonic speeds.

It has been found that over wide ranges of subsonic vehicle operating conditions the solutions of the conservation equations, formulated for steady flow in the reference frame of the vehicle, have notable properties. Foa[2], assuming a unique heat transfer schedule, has shown that, for $M_V < 1/\sqrt{\gamma}$, the only steady-flow solution that is possible is one in which the flow is at rest (relative to the tube) everywhere downstream of a station a finite distance from the vehicle. Hagerup[3] and Schmid[4], using linearized analyses neglecting dissipation, have indicated that the flow behind a subsonic vehicle will reach its appropriate downstream boundary condition only if the pressure is constant and the velocity and enthalpy perturbations in the wake region are identical ($\sigma/\sigma_f = T/T_o$ in the present notation). In a more recent study, including nonlinear effects, Schmid[5] has shown that the constant pressure condition does not apply exactly but that there is still a restricted regime of related velocity and enthalpy distributions which permit a steady flow solution.

The present study is an analysis of the effects of friction and heat transfer on the nonsteady flow field induced by a subsonic vehicle traveling in an infinite tube. The purpose of this study is to determine whether there is any trend towards steadiness in the vehicle-fixed coordinate system and, if so, to compare the resulting flow field with the steady-flow solutions previously obtained. The analysis is carried out by a simulation technique analogous to that used in Ref. 1, where a

detonation is used to generate a flow field simulating that induced by an internally-propelled supersonic vehicle. In the present study the simulating disturbance is a heat source moving at a constant subsonic speed.

Description of the Model

A supersonic vehicle in steady motion can be simulated by a Chapman-Jouguet detonation (Ref. 1) because the Chapman-Jouguet condition insures a constant propagation velocity. In contrast, a deflagration propagating through a combustible mixture in a duct is a distinctly non-steady phenomenon.[6,7,8] Turbulence within the flow field distorts and accelerates the flame front so that the propagation velocity is not constant. If the mixture is within the detonable limits a detonation will form when the flame catches up with the shock formed at ignition, or when this shock is strengthened by flame-generated compression waves and becomes strong enough to ignite the mixture. Therefore a deflagration cannot be used to simulate a vehicle traveling subsonically at constant speed.

In order to simulate a subsonic vehicle in steady motion the following model is considered. One half of an infinite tube is filled with a combustible mixture and the other half is filled with an inert gas (Figure 1). A constant-velocity flame is produced using a steady burning fuse or firing a series of spark plugs in succession along the tube walls. The decrease in chemical energy during combustion has the same effect on the adjacent flow field as heat released by a one dimensional heat source traveling at constant velocity through the tube. The term "heat source" will be used from here on in order to distinguish this model from a deflagration.

On ignition, a forward-facing shock 1 starts traveling through the mixture while a rearward-facing shock 2 starts propagating through the inert gas (Figure 2). An interface between burned and inert gas also travels through the duct.

The following assumptions are made:

1) The heat source is a one-dimensional discontinuity across which the flow is quasi-steady, i.e., the transformation across the flame behaves at each instant as a steady flow with the same instantaneous boundary conditions.

2) The time rate of heat release of the heat source is constant. This assumption, which is not valid for an accelerating deflagration, simulates the heat release of an internally-propelled vehicle in steady motion. Due to the forward-facing shock, the gas ahead of the flame is in motion. Dissipative effects will alter this motion, and the mass rate of flow and heat release per unit mass across the flame will be time dependent. The product of these two parameters is, however, invariant with respect to time, by virtue of the assumption that the time rate of heat release is constant. (This assumption is automatically satisfied in detonative combustion, where there is no pre-disturbance of the flow field, and the mass rate of flow and the heat release per unit mass are therefore both constant).

3) The flow is one-dimensional, fully developed, and turbulent in the entire flow field between the forward and rearward-facing shocks.

4) The gases are ideal and the ratio of specific heats is constant throughout the flow field.

5) The duct is of infinite length.

The induced flow field is analyzed by the method of characteristics for one dimensional nonsteady flow with consideration of friction

and heat transfer.

Although idealized, this model is capable of revealing the essential features of dissipation in the flow field generated by an internally propelled vehicle traveling subsonically in a duct, and of detecting any trend towards steadiness in a vehicle-fixed frame of reference.

2. EQUATIONS OF MOTION

The characteristic equations for one-dimensional nonsteady flow including friction and convective heat transfer have been derived in Reference 1.

They are:

$$\frac{\delta_+ P}{\delta \tau} = -\frac{C_f |U|}{\pi A}\left[A^2 - \left(\frac{\gamma-1}{2}\right)U^2 - 1 + UA\right] + A\frac{\delta_+ S}{\delta \tau}, \qquad (1)$$

$$\frac{\delta_- Q}{\delta \tau} = -\frac{C_f |U|}{\pi A}\left[A^2 - \left(\frac{\gamma-1}{2}\right)U^2 - 1 - UA\right] + A\frac{\delta_+ S}{\delta \tau}, \qquad (2)$$

$$\frac{DS}{D\tau} = -\frac{C_f |U|}{\pi(\gamma-1)A^2}\left[A^2 - \left(\frac{\gamma-1}{2}\right)U^2 - 1\right] \qquad (3)$$

In the previous report heat has been assumed to be transferred only by convection, but in the present study the above equations are modified to account for conductive heat transfer effects.

In a steady-flow analysis of the vehicle wake,[9] Cromack has found that unless conductive heat transfer is also accounted for, the pressure and temperature never return to ambient conditions. This difficulty is not encountered in nonsteady flows, since if the flow does come to rest before ambient conditions have been attained, nonsteady waves set the flow in motion again and convective heat transfer will again occur. However, to facilitate comparison with results of steady-flow analyses, conduction is included in the present nonsteady-flow analysis.

The entropy change due to heat transfer is

$$\frac{Dq}{Dt} = -\frac{2h}{\rho R T}\left(T^\circ - T_0\right) \qquad (4)$$

Let $h = h_1 + h_2$ where h_1, the film coefficient of convective heat transfer, is related to the friction factor by Reynolds analogy,[10]

$$h_1 = \frac{C_f}{2} \rho C_p |u| \tag{5}$$

and h_2 is the film coefficient of conductive heat transfer;

$$h_2 = K \frac{C_f}{2} \rho C_p |u_f - u| \tag{6}$$

This form is chosen for h_2 so that it will be dimensionally consistent with h_1, and also so that h_2 will be constant for steady flow in a vehicle fixed coordinate system. (Note: $\rho |u_f - u|$ is proportional to the mass rate of flow in such a coordinate system). K is a small multiplier chosen so that the conductive heat transfer is of the correct order of magnitude for the gas at rest.

With the inclusion of conduction the characteristic equations become

$$\frac{\delta + P}{\delta \tau} = -\frac{C_f |U|}{\bar{r} A} \left[A^2 - \left(\frac{\gamma-1}{2}\right) U^2 - 1 + U A \right] \tag{7}$$
$$- \frac{K C_f}{\bar{r} A} |U_f - U| \left[A^2 + \left(\frac{\gamma-1}{2}\right) U^2 - 1 \right] + A \frac{\delta + S}{\delta \tau} ,$$

$$\frac{\delta - Q}{\delta \tau} = -\frac{C_f |U|}{\bar{r} A} \left[A^2 - \left(\frac{\gamma-1}{2}\right) U^2 - 1 - U A \right] \tag{8}$$
$$- \frac{K C_f}{\bar{r} A} |U_f - U| \left[A^2 + \left(\frac{\gamma-1}{2}\right) U^2 - 1 \right] + \frac{\delta - S}{\delta \tau} ,$$

and

$$\frac{DS}{D\tau} = -\frac{C_f |U|}{\bar{r}(\gamma-1) A^2} \left[A^2 - \left(\frac{\gamma-1}{2}\right) U^2 - 1 \right] \tag{9}$$
$$- \frac{K C_f}{(\gamma-1) \bar{r} A^2} |U_f - U| \left[A^2 + \left(\frac{\gamma-1}{2}\right) U^2 - 1 \right]$$

Equations (7), (8) and (9) are integrated along their respective characteristics in order to determine the nonsteady flow field.

3. RESULTS

Equations (7), (8) and (9) have been integrated numerically using a finite difference technique on the IBM Systems 360 Computer. They have been solved both for an inviscid adiabatic case and for a case involving friction and heat transfer.

Results for Inviscid Adiabatic Flow

When the flow is inviscid the adiabatic and right-hand side of each of equations (7), (8) and (9) is zero, hence P and Q are constant along their respective characteristics and S is constant along the particle pathline. The solution for this situation is outlined in Appendix I. Results for a case in which the vehicle velocity is $U_f = 0.5$ and the heat release per unit mass is $J = 12.045$ are presented in Table I. The wave diagram for this case is presented as Figure 3.

From the analysis in Appendix 1 and the results in Table I it can be seen that the inviscid adiabatic flow field is uniform in the region between shock 1 and the heat source front, and then again in the region between the rear of the heat source and the interface. Therefore in these regions the flow is steady in a frame of reference moving with the heat source. Since shock 1 and the interface are moving further away from the heat source, this region of steady flow grows as time progresses.

It is interesting to compare this phenomenon with its counterpart in the supersonic case (Reference 1), where, because of an expansion wave behind the detonation, the inviscid adiabatic flow field is nonsteady in the detonation-fixed coordinate system. In the subsonic case this expansion wave is not present and the flow is steady.

Since dissipation has not been included, this analysis yields a

flow that never returns to ambient conditions. On the other hand, when friction and heat transfer are accounted for, this flow field is modified as described in the following section.

Results for Case Involving Friction and Heat Transfer

Equations (7), (8) and (9) have also been solved with consideration of the effects of friction and heat transfer. A finite difference technique has been used to integrate these equations numerically under the following conditions:

$$C_f = 0.01 \,, \; r = 2 \text{ in.} \,, \; \gamma = 1.4 \,, \; K = 0.0002$$

$$h_o = 5.28 \text{ ft.} \,, \; U_f = 0.5 \,, \; \dot{J} = 3.19 \,.$$

The construction of the characteristic network and the details of the integration technique are described in Appendices 2 and 3. The wave diagram for this case is shown on Figure 3.

Since for short initial time intervals the integrated effects of friction and heat transfer are small, the initial flow field is substantially that predicted by the inviscid adiabatic analysis. Therefore at early values of time the flow can be said to be steady in a coordinate system moving with the heat source.

Figures 4, 5 and 6 show the velocity, temperature and pressure distributions in the wake region, in a coordinate system moving with the heat source. In these figures ξ represents distance from the heat source.

Initially the distributions are uniform. As time progresses, the effects of friction and heat transfer cause an increase in the velocity (Fig. 4) and a corresponding increase in the convective heat transfer rate, at any point a fixed distance from the heat source. Furthermore the

convective heat transfer rate is always higher close to the heat source than further downstream. Therefore at any instant fluid particles at a relatively short distance from the heat source are at a lower temperature than particles further downstream; hence the minimum in the curves of Figure 5.

It should be noted that Figure 5 only represents the wake region between the heat source and the interface. The curves terminate at the interface, where the temperature drops discontinuously.

Since the pressure, velocity and temperature distributions vary continually with time, the flow field has become nonsteady in a frame of reference moving with the heat source. Friction and heat transfer have modified the initially steady flow field to one that is nonsteady.

This is the direct opposite of the result obtained in Reference 1 for the supersonic case, where friction and heat transfer were found to change the initially nonsteady flow field to one that was steady in a frame of reference moving with the detonation front.

Since the detonation travels at supersonic velocity relative to the wake region,* downstream disturbances traveling at sonic speed can never reach the detonation from behind. As time progresses, friction and heat transfer decrease both the velocity and the speed of sound in the wake region and therefore sweep the similarly facing characteristics away from the detonation (Reference 1, Figure 5). This results in the generation of an ever growing region of flow moving along with the detonation which is completely isolated from the time-dependent downstream flow conditions. Since the conditions ahead of the detonation are time independent,

---

* Except immediately behind the detonation where the relative flow velocity is sonic, due to the Chapman-Jouguet condition.

this region of the flow is steady in a frame of reference fixed to the detonation front.

The subsonic heat source, on the other hand, travels at subsonic velocity relative to the wake region, and downstream disturbances can overtake it from behind. As the flow field far downstream gradually returns to ambient conditions, signals travel upstream and continually alter the flow directly behind the heat source. Dissipation also causes a timewise variation of the predisturbed flow field ahead of the source.

It can be seen from Figures 4, 5 and 6 that the flow field seems to be approaching an asymptotic condition as time progresses (e.g., the velocity distribution changes much less between $\tau = 40$ and $\tau = 80$ than it does between $\tau = 10$ and $\tau = 20$). If this trend continues, a point will be reached when the timewise variation of the flow field will be imperceptible and the flow will be substantially steady. Unlike the supersonic case, where a region of steady flow develops immediately behind the vehicle, in the subsonic case steady flow is approached gradually throughout the entire flow field as the nonsteady effects slowly decay.

Although at $\tau = 80$ the flow is not yet exactly steady, it will be shown that the distributions calculated for this value of τ are in close correlation with previously obtained steady flow solutions.

In Figure 4 it is noted that at $\tau = 80$, $\xi = 40$ the nondimensional flow velocity relative to the wall has decayed to 0.015. This is in good agreement with Foa's conclusion that the flow must return to rest relative to the tube a finite distance from the vehicle.

Figure 7 shows T/T_o and ρ/ρ_f in the wake region at various values of τ. As before, these distributions are in a coordinate system moving with the heat source, and ξ represents distance from the heat source.

It can be seen that as time progresses these two families of curves are slowly approaching each other. When the flow finally becomes exactly steady the two distributions will probably not coincide as this would require constant pressure throughout the entire wake region (in Figure 6 it can be seen that even at $\tau = 80$ there is still a pressure variation). However, an asymptotic condition is approached which seems to be close to that predicted by the linearized analyses of Hagerup and Schmid (i.e., $T/T_o = v/v_f$).

Schmid has also shown that the distributions at $\tau = 80$ are within the restricted regime where steady flow solutions are possible. One of these solutions has recently been obtained numerically[5] using the apparent asymptotic conditions immediately behind the heat source as initial values. These results are indicated on Figures 4 and 5. It can be seen that the results of the present analysis are in good agreement with the steady flow solution.

Figure 8 shows the pressure, temperature and velocity distributions ahead of the heat source at $\tau = 80$. These distributions are in a coordinate system fixed to the heat source, but in this case ξ represents distance measured ahead of the heat source. A comparison of these results with those of steady-flow analyses is impossible at this writing because, due to numerical instabilities, steady flow solutions for the region ahead of the vehicle have not yet been obtained.

4. CONCLUSIONS

The flow field induced in an infinite tube by a subsonic internally propelled vehicle is qualitatively similar to that generated by a subsonically moving heat source. Therefore the following conclusions apply qualitatively to the case of the vehicle as well as to the case of the heat source.

When a subsonic heat source is initiated in an infinite tube the resulting flow field goes through three distinct stages before it reaches its final state. Initially the integrated effects of friction are small and the flow is substantially steady in a coordinate system moving with the heat source. Friction and heat transfer soon modify the initially steady flow to one that is nonsteady in this frame of reference. As time progresses, the nonsteady effects slowly decay and the flow field approaches a time-invariant asymptote. In this final steady state the calculated distributions are very close to those predicted by the steady-flow solution.

5. APPENDICES

APPENDIX I

Solution for Inviscid and Adiabatic Flow

The steady flow equations for a one dimensional heat source traveling into a gas in motion are:

Continuity: $$\rho_u (u_f - u_u) = \rho_b (u_f - u_b) \tag{A-1}$$

Momentum: $$\rho_u (u_f - u_u)^2 + p_u = \rho_b (u_f - u_b)^2 + p_b \tag{A-2}$$

Energy: $$c_p T_b + \frac{(u_f - u_b)^2}{2g} = c_p T_u + \frac{(u_f - u_u)^2}{2g} + J \tag{A-3}$$

Nondimensionalizing the terms, using the perfect gas law and the definition of the speed of sound, these equations can be put in the following form.

$$U_b = \frac{1}{\gamma+1}\left\{-\left[\frac{A_J^2}{U_f - U_J} - U_f - \gamma U_J\right] + \sqrt{-\bar{J} + \left[\frac{A_J^2}{U_f - U_J} - (U_f - U_J)\right]^2}\right\} \tag{A-4}$$

$$A_b = A_u \sqrt{\left[1 + \frac{\gamma}{A_J^2}(U_f - U_J)(U_b - U_J)\right]\left[\frac{U_f - U_b}{U_f - U_J}\right]} \tag{A-5}$$

$$\frac{p_b}{p_u} = 1 + \frac{\gamma}{A_u^2}(U_f - U_J)(U_b - U_J) \tag{A-6}$$

Therefore if the flow conditions ahead of the heat source are known along with U_f and $\bar{J}$, all of the flow conditions behind the heat source can be calculated. U_f the nondimensionalized heat source velocity was chosen as .5 and $\bar{J}$ the nondimensionalized heat release per unit mass was chosen as 12.04.

Due to the forward facing shock (shock 1) the flow conditions immediately ahead of the heat source are not known a priori. Therefore

the following iteration procedure is used.

A first approximation to the Mach number of shock 1 is guessed at. Then using the shock equations (Reference 1, Appendix 1) a first approximation is obtained for the flow conditions immediately behind shock 1. Since between shock 1 and the source front the flow field is uniform a first approximation to the flow conditions ahead of the heat source is therefore known. Equations (A-4), (A-5) and (A-6) are then solved for a first approximation to the flow conditions behind the heat source.

Between the rear of the heat source and the interface the flow field is uniform, but across the interface there is a discontinuous jump in temperature and entropy. Between the left side of the interface and shock 2 the flow field is uniform. Since the pressure and velocity do not change across the interface a first approximation to these two parameters behind shock 2 is known.

The pressure and velocity behind a shock, propagating into a flow at rest, independently determine the shock Mach number. Therefore if the pressure and velocity obtained by the above procedure do not correspond to the same Mach number M_{s2}, the first approximation for M_{s1} is in error. Therefore M_{s1} is modified until the pressure and velocity behind shock 2 yield the same Mach number M_{s2} and the flow field is uniquely determined.

APPENDIX 2

Construction of the Characteristic Grid

A sketch of the characteristic grid for when friction and heat transfer are included can be found on Figure 9.

At early values of τ the effect of friction and heat transfer is negligible. Therefore the inviscid adiabatic solution can be used as initial conditions at points 1-7 on Figure 9. The location of these points is arbitrary provided that τ is small. These points were uniformally distributed along the flow field at $\tau = 1$.

For the supersonic detonation (Reference 1), the Chapman-Jouguet condition immediately behind the detonation serves as a boundary condition for all time. For the subsonic heat source the corresponding boundary condition is the satisfaction of the quasi-steady conservation equations across the heat source (with constant u_f and $\dot{J}$). The procedure used to impose this boundary condition (at points such as F') is outlined in Appendix 3.

The construction of the characteristic network is exactly the same as for the supersonic case and is described in Appendices 2 and 3 of Reference 1. The solution for the instances when a characteristic crosses as interface or a shock (points S', S'', I') is described in Appendices 3B and 3C of Reference 1.

APPENDIX 3

Solution When Characteristics Cross the Heat Source (Figure 10)

Points 1 and 2 are two points in the time distance plane at which all flow conditions are known. Point 3 is a point along the heat source. The flow conditions are known at both sides of the heat source at 3 (subscripts 3a and 3b represent conditions immediately ahead of and behind the heat source respectively).

In this case the Q characteristic from point 1 must cross the heat source at point 4 before it intersects the P characteristics from point 2. The following procedure is used to determine the location and flow conditions at point 4.

Assume as a first approximation that the flow conditions at point 4 are the same as at point 3. Then the Q characteristic is extended with the average slope between points 1 and 4a . The heat source is extended with slope $1/U_f$. The intersection of these two lines determines a first approximation to the location of point 4.

The P characteristic and particle pathline through point 4 originate at points 5 and 6. The procedure used to determine the locations of these points isdescribed in Appendix 3A Reference 1.

Higher approximations to the flow conditions at point 4 are made in the following manner. Equations (7), (8), and (9) are rewritten

$$P_{4b} - P_5 = \left\{ -\frac{C_f|U|}{\bar{\pi} A}\left[A^2 - \left(\frac{\gamma-1}{2}\right)U^2 - 1 + UA\right] - \frac{KC_f|U_f-U|}{\bar{\pi} A}\left[A^2 + \left(\frac{\gamma-1}{2}\right)U^2 + -1\right]\right\}_{4b,5}(P_4 - P_5) + A_{4b,5}(S_{4b} - S_5) \quad \text{(A-7)}$$

$$Q_{4a} - Q_1 = \left\{ -\frac{C_f|U|}{\bar{\pi} A}\left[A^2 - \left(\frac{\gamma-1}{2}\right)U^2 - 1 - UA\right] - \frac{KC_f|U_f-U|}{\bar{\pi} A}\left[A^2 + \left(\frac{\gamma-1}{2}\right)U^2 + -1\right]\right\}_{4a,1}(P_4 - P_1) + A_{4a,1}(S_{4a} - S_1) \quad \text{(A-8)}$$

$$S_{4a} - S_6 = \left\{ -\frac{C_f|U|}{\bar{\pi}(\gamma-1)A^2}\left[A^2 - \left(\frac{\gamma-1}{2}\right)U^2 - 1\right] - \frac{KC_f|U_f-U|}{\bar{\pi}(\gamma-1)A^2}\left[A^2 + \left(\frac{\gamma-1}{2}\right)U^2 - 1\right]\right\}_{4a,6}(P_4 - P_6) \quad \text{(A-9)}$$

Subscript 1,4 means that the flow parameters are averaged between points 1 and 4.

Equations (A-7), (A-8) and (A-9) are solved for S_{44}, Q_{44} and P_{46} using the previous approximation to evaluate the right hand side. The remaining flow parameters are determined using the quasi-steady equations across the flame for constant U_f and $\dot{J}$. (Equations A-4, A-5, A-6). The following iteration procedure is used.

U_{44} is guessed at, and A_{44} and $\left(\rho_{44}/\rho_0\right)\left(S_{44}/a_0\right)$ are calculated.

$$A_{44} = \left(Q_{44} + U_{44}\right) / \left(\frac{\gamma-1}{2}\right)$$

$$\left(\frac{\rho_{44}}{\rho_0}\right)\left(\frac{S_{44}}{a_0}\right) = \left(\frac{\rho_{44}}{\rho_0}\right)\left(U_f - U_{44}\right) = \left(A_{44}\right)^{2/\gamma-1} e^{-S_{44}}\left(U_f - U_{44}\right)$$

Therefore since $\bar{J} = \left(\frac{\rho_0}{\rho_{44}}\right)\left(\frac{a_0}{S_{44}}\right)\dot{J}$, $\bar{J}$ can be calculated.

Then using the quasi steady equations A_{46} and U_{46} are determined. If these values do not combine to form P_{46} the first guess for U_{44} must be modified until the flow conditions across the heat source are uniquely determined.

This iteration is continued until the difference between two successive approximatiors converges to the desired accuracy.

6. REFERENCES

1. Skinner, J.H., "Plane Flame Simulation of the Wake Behind an Internally Propelled Vehicle -- Part I - Simulation of a Supersonic Vehicle by a Detonation," Rensselaer Polytechnic Institute, TR AE 6701, Troy, New York, March 1967.

2. Foa, J.V., "Propulsion of a Vehicle in a Tube," Rensselaer Polytechnic Institute, TR AE 6404, Troy, New York, June 1964.

3. Hagerup, H.J., "A Note on the Flow Induced by a Disturbance Traveling in a Tube," Rensselaer Polytechnic Institute, TR AE 6405, Troy, New York, June 1964.

4. Schmid, J.R., "Linearized Analysis of the Flow Field Induced by a Small Disturbance Propagating Through an Infinite Tube," Rensselaer Polytechnic Institute, TR AE 6706, Troy, New York, to be submitted.

5. Schmid, J.R., "Steady-Flow Simulation Study of the Disturbance Produced by an Internally Propelled Vehicle in an Infinite Tube -- Subsonic Vehicle," Rensselaer Polytechnic Institute, TR AE 6707, Troy, New York, to be submitted.

6. Bone, W.A., Fraser, R.P., and Wheeler, W.H., "A Photographic Investigation of Flame Movements in Gaseous Explosions," Transactions of the Royal Society, A, 235, p. 29, London, 1936.

7. Taylor, G.I., and Tankin, R.S., "Gas Dynamical Aspects of Detonation," Fundamentals of Gas Dynamics, Princeton University Press, New Jersey, 1958, Chap. 3.

8. Foa, J.V., Elements of Flight Propulsion, John Wiley and Sons, New York, 1960, Chap. 11, p. 249.

9. Cromack, D.E., "Steady-Flow Simulation Study of the Disturbance Produced by an Internally-Propelled Vehicle in an Infinite Tube -- Supersonic Vehicle," Rensselaer Polytechnic Institute, TR AE 6704, Troy, New York, June 1967.

10. Rohsenow, W.M. and Choi, H.Y., Heat Mass and Momentum Transfer, Prentice Hall, New York, 1961.

TABLE 1

Results for Inviscid Adiabatic Flow

$U_f = 0.5$ $\quad \bar{J} = 12.04$ $\quad \dot{J} = 3.19$

Location	U	A	p/p_o	S	Slope
Behind Shock L	0.305	1.062	1.513	0.005	$M_{s1} = 1.2$
Ahead of Heat Source	0.305	1.062	1.513	0.005	$U_f = 0.5$
Behind Heat Source	-0.206	1.894	1.326	2.993	$U_f = 0.5$
Right Side of Interface	-0.206	1.894	1.326	2.993	$U = -.206$
Left Side of Interface	-0.206	1.041	1.326	.001	$U = -.206$
Behind Shock 2	-0.206	1.041	1.326	.001	$M_{s2} = 1.131$

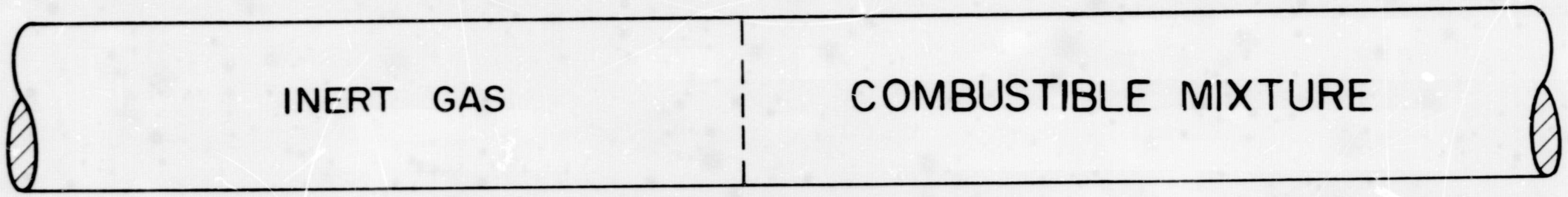

FIGURE 1. Gases at rest before ignition

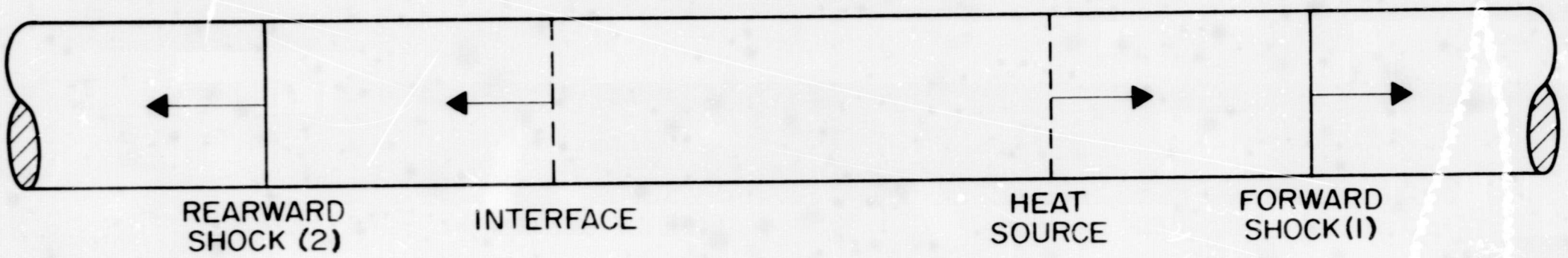

FIGURE 2. Situation after ignition

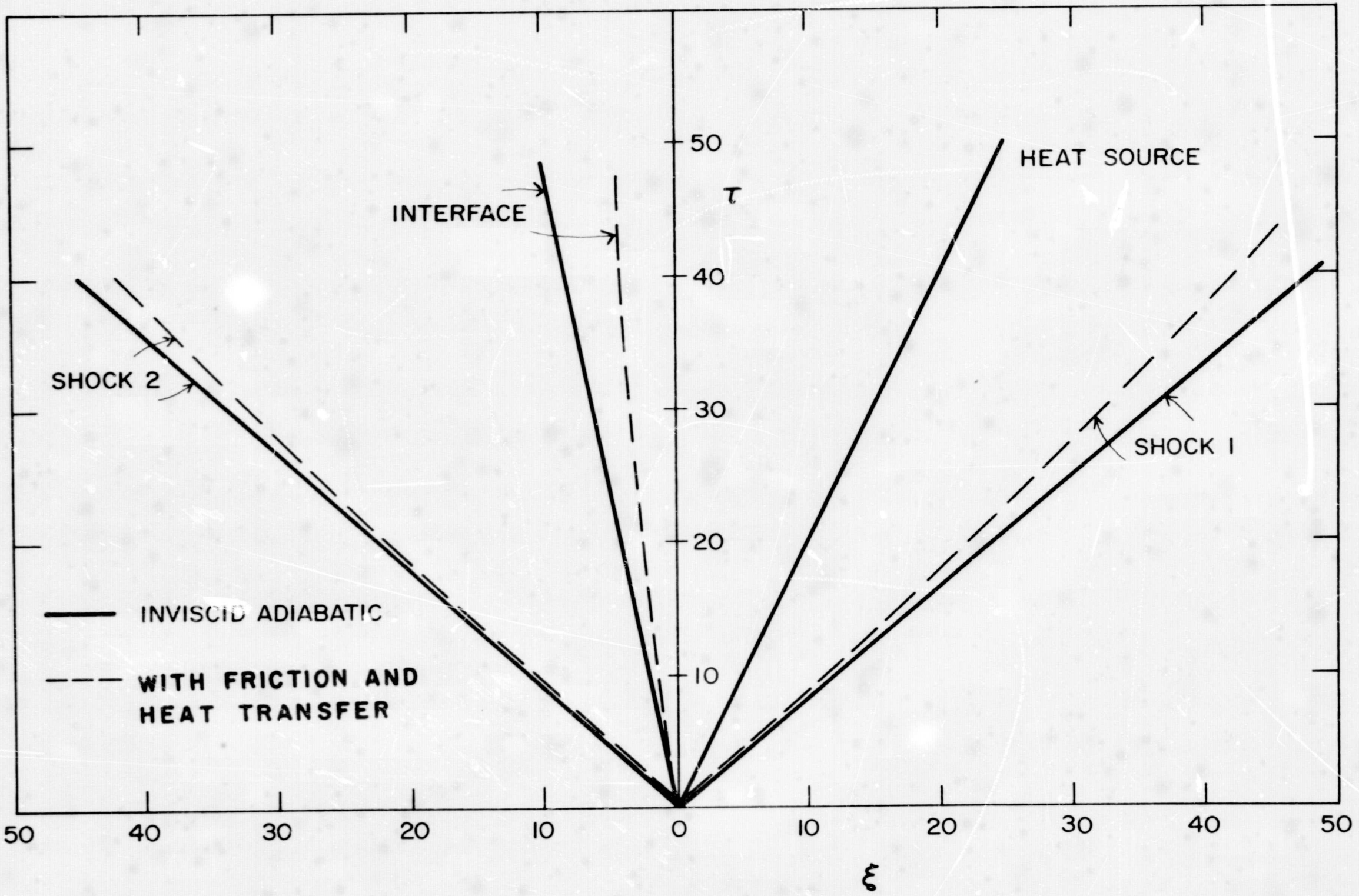

FIGURE 3. Wave diagram for inviscid adiabatic flow and for flow with friction and heat transfer

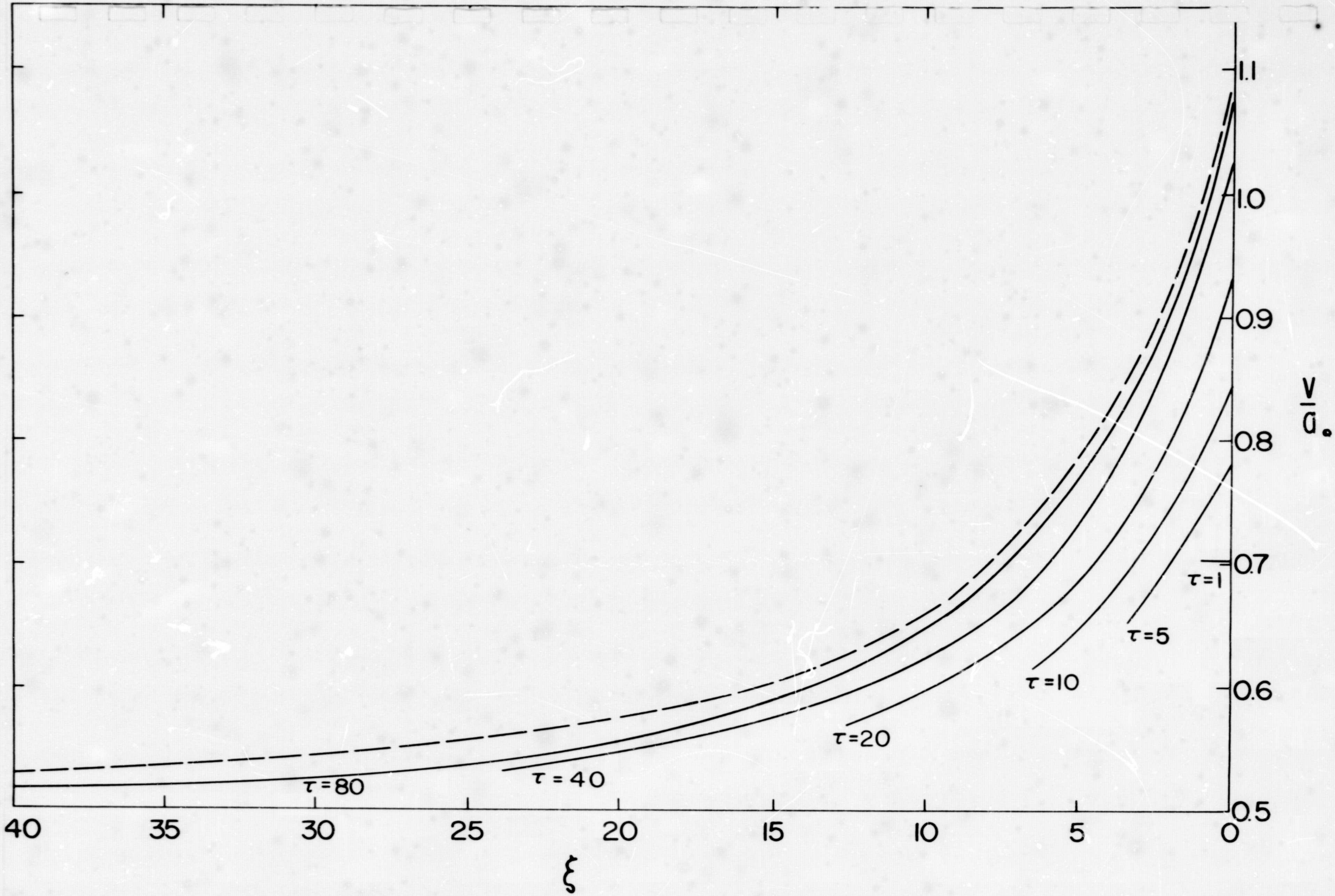

FIGURE 4. Velocity distribution in the wake region in a coordinate system fixed to the heat source (dotted line is the steady-flow solution from Ref. 5)

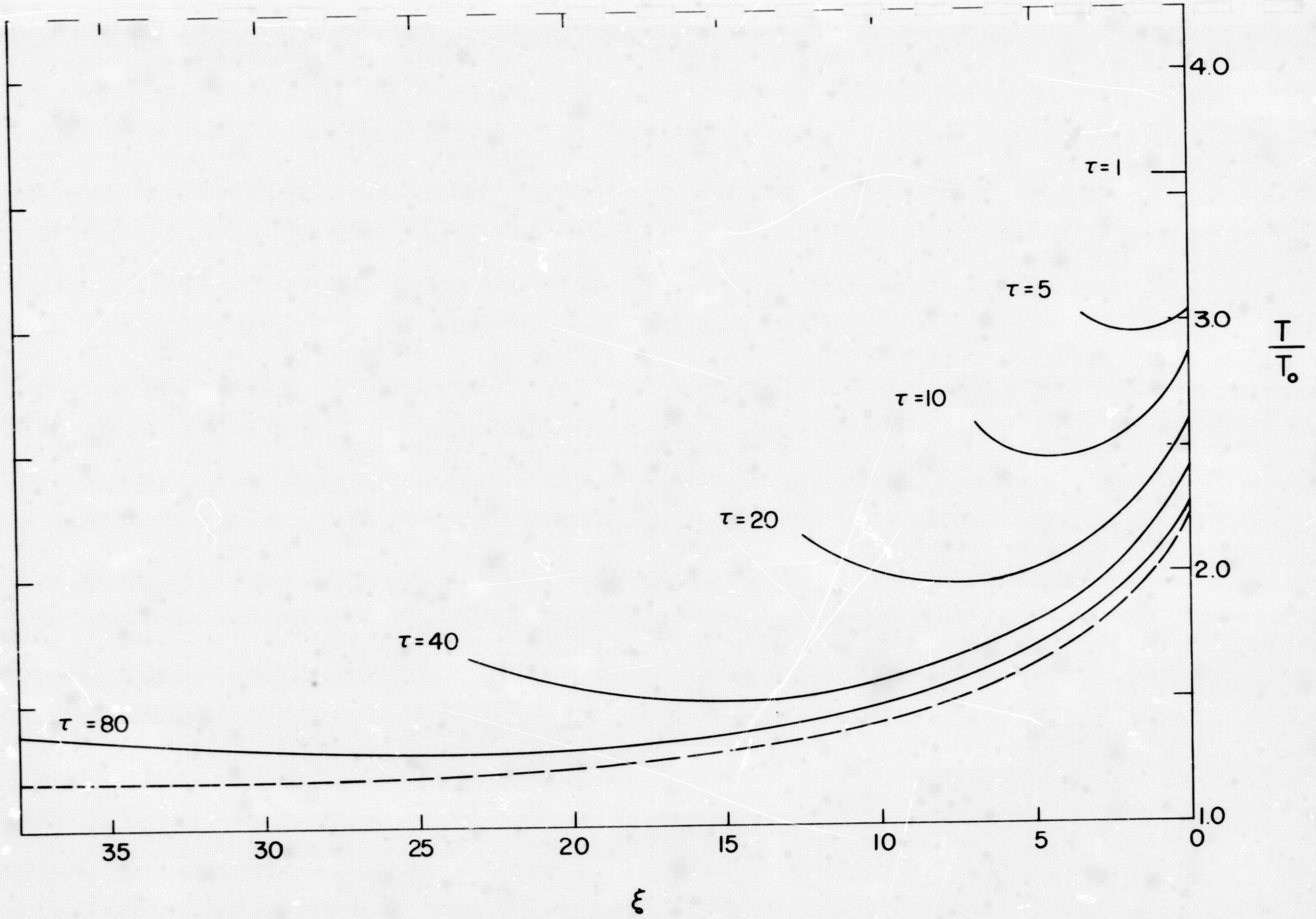

FIGURE 5. Temperature distribution in the wake region in a coordinate system fixed to the heat source (dotted line is the steady-flow solution from Ref. 5)

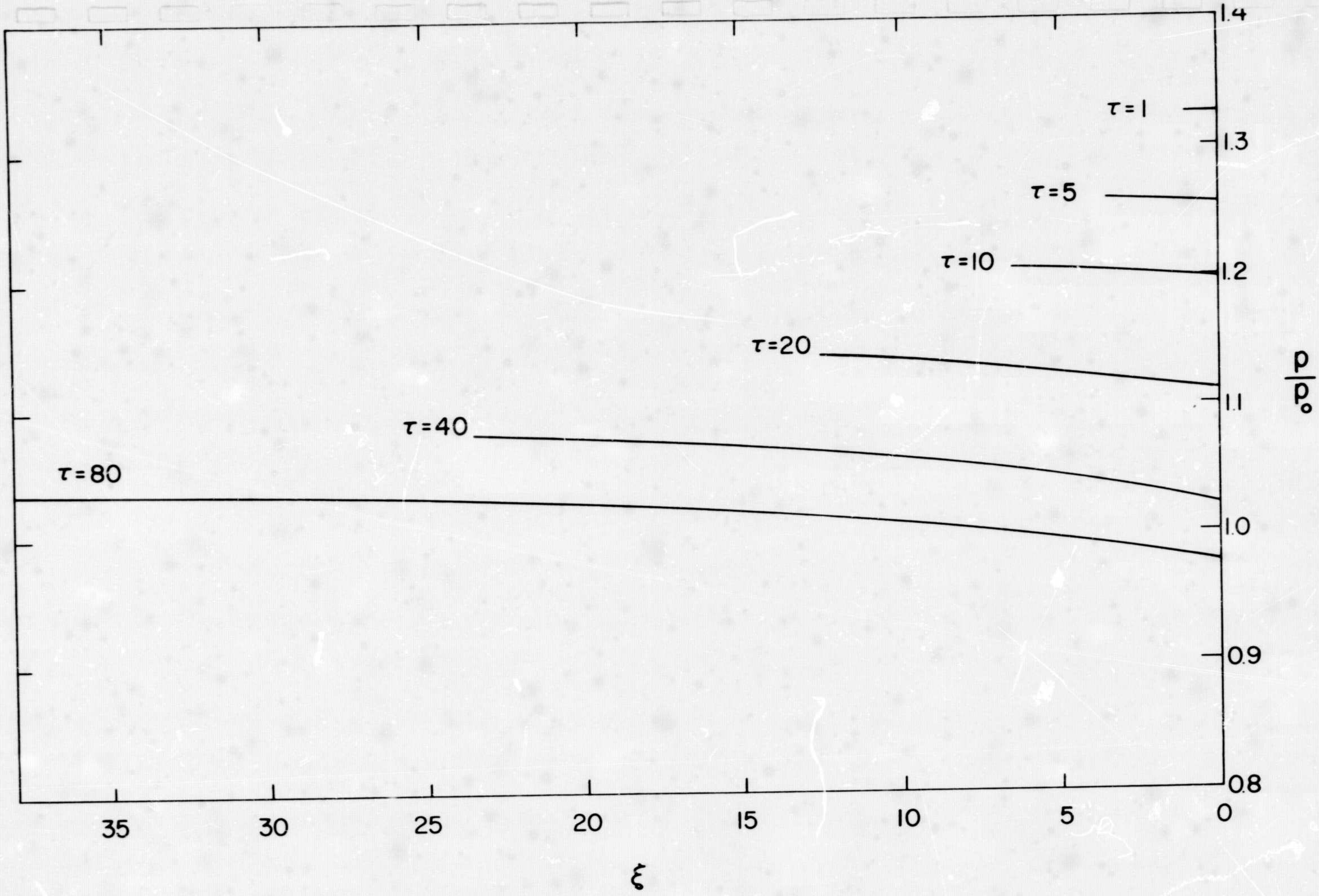

FIGURE 6. Pressure distribution in the wake region in a coordinate system fixed to the heat source

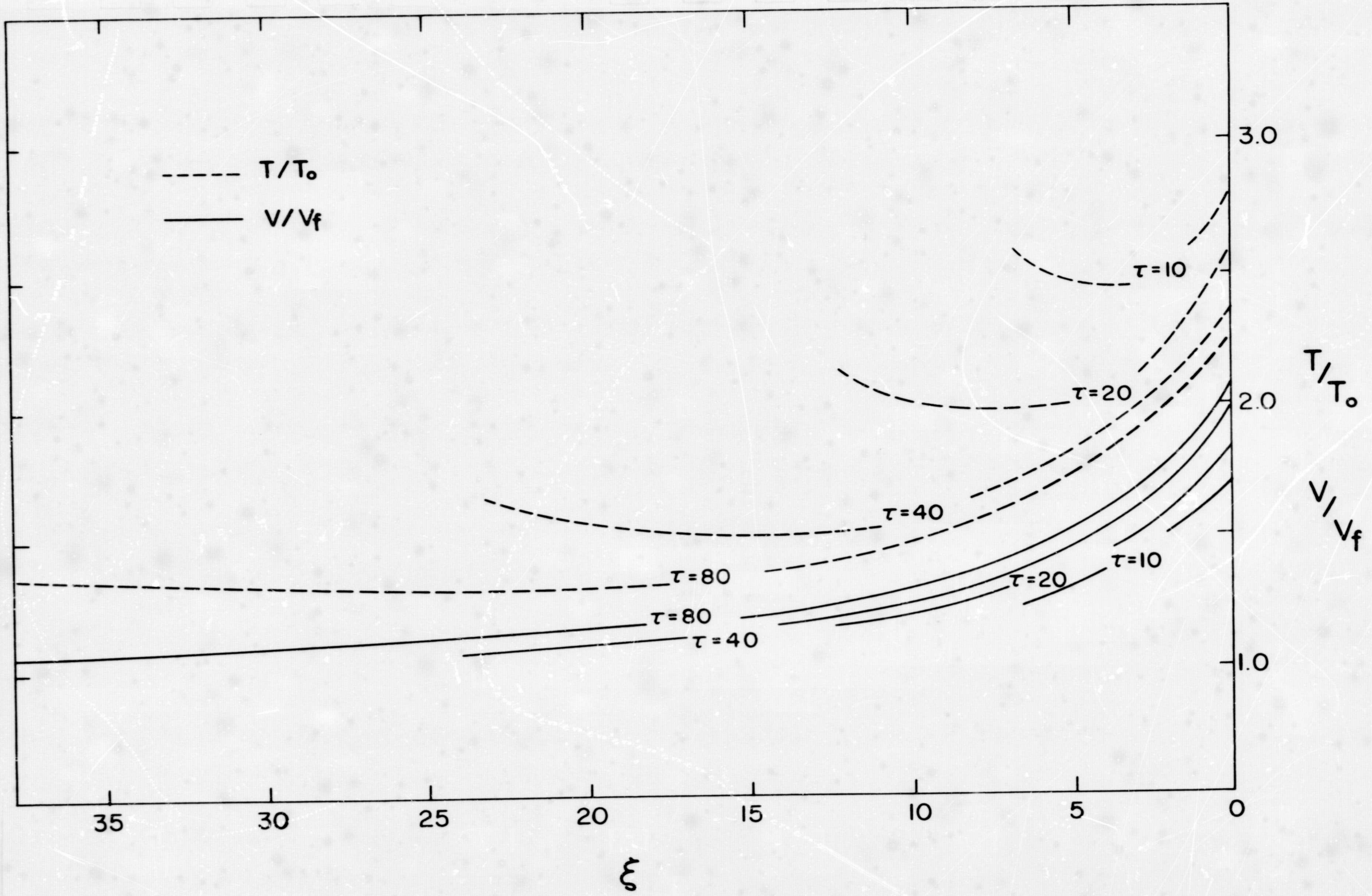

FIGURE 7. Timewise variation of T/T_o and v/v_f in the wake region in a coordinate system moving with the heat source

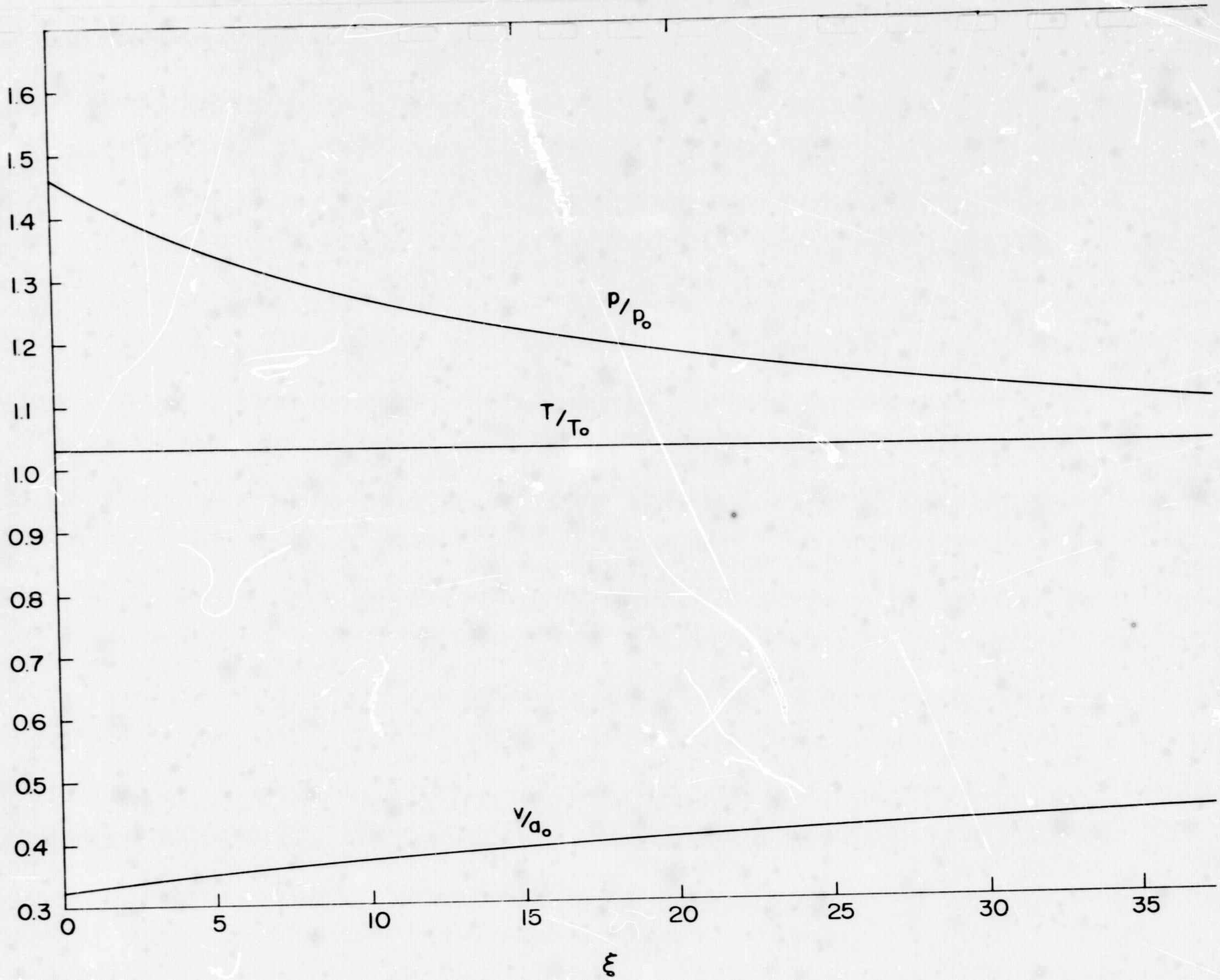

FIGURE 8. Pressure, temperature and velocity distributions ahead of the heat source at $\tau = 80$ in a co-ordinate system fixed to the heat source

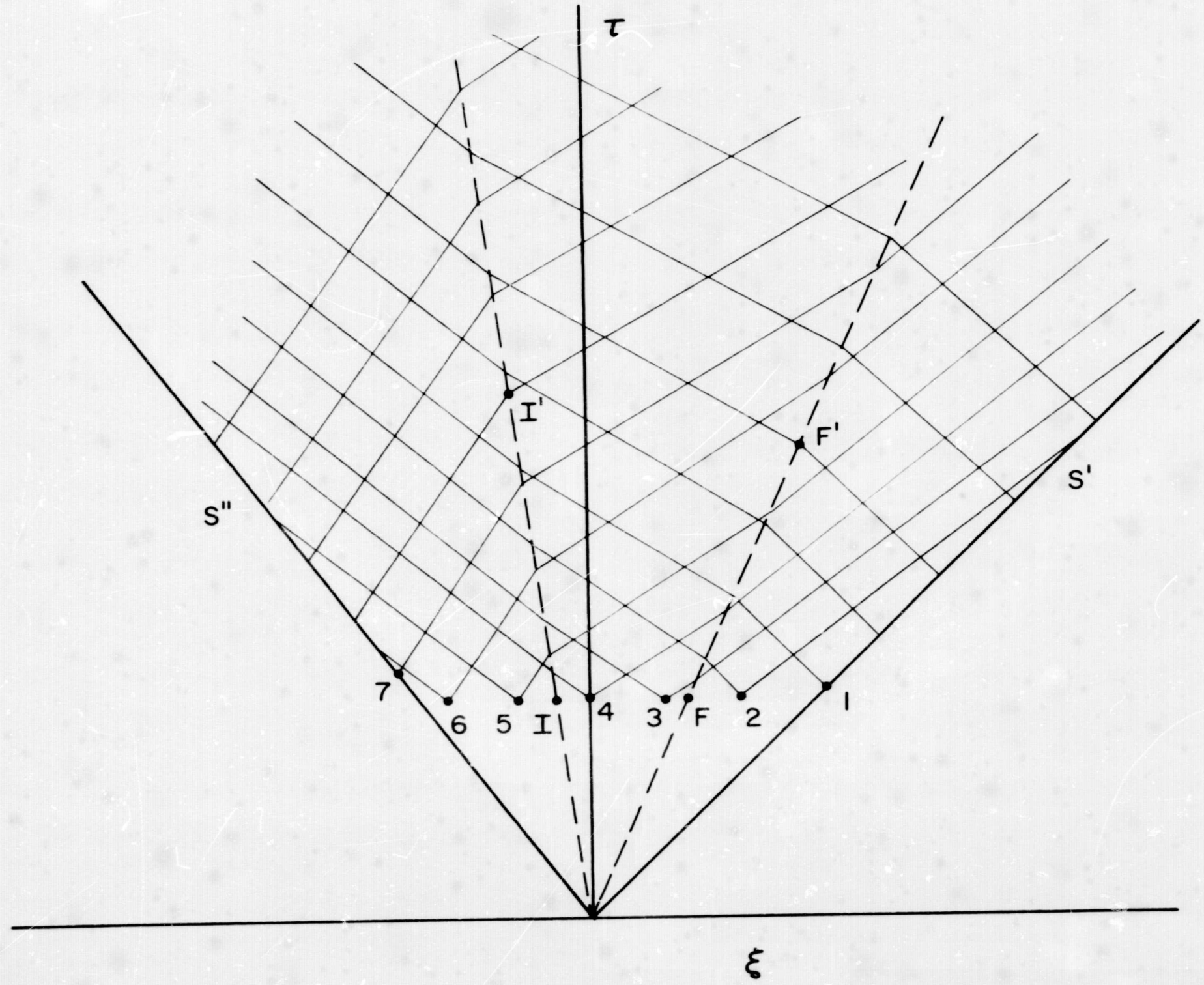

FIGURE 9. Construction of characteristic grid

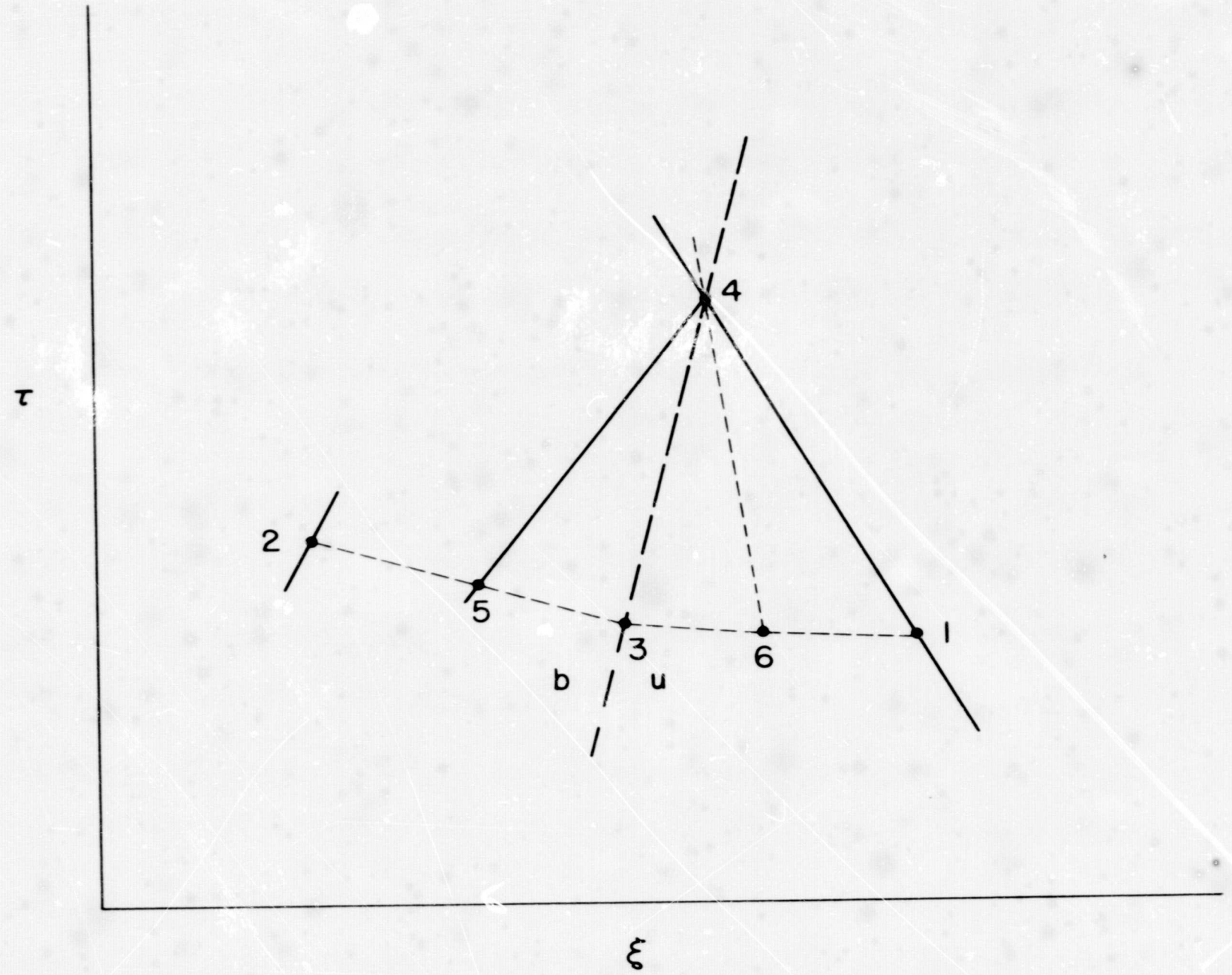

FIGURE 10. Solution for a characteristic crossing heat source